

# REDUCTION OF GPS STANDARD RECEIVERS NOISE USING PARALLEL-STRUCTURE WAVELET BASED NEURAL NETWORKS

M. R. Mosavi

Department of Electrical Engineering, Behshahr University of Science and Technology, Behshahr 48518-78413, Iran

Email: M\_Mosavi@iust.ac.ir

**KEY WORDS:** Reduction, Noise, GPS, Parallel-Structure, Wavelet, Neural Networks

## ABSTRACT:

Position information obtained from standard GPS receivers is known to be corrupted with noise. To make effective use of GPS information in a navigation system it is essential to model this noise and to eliminate its effect. This paper present Parallel Structure Wavelet Based Neural Network (PSWNN) for predicting the Differential GPS (DGPS) corrections. The PSWNN consists of multiple numbers of WNNs connected in parallel. Each WNN in the PSWNN predicts the same DGPS corrections future value based on input data with different embedding dimension and time delay. The embedding dimension is chosen optimally to have superior performance for each time delay value. The PSWNN determines the final predicted value by averaging the outputs of each WNN.

The performance of proposed PSWNN is compared with WNN in application of DGPS corrections prediction. The proposed algorithms in DGPS system are implemented by a low cost commercial Coarse/Acquisition (C/A) code GPS module. The experimental results demonstrate which the PSWNN has great approximation ability and suitability in DGPS connection prediction than WNN; so that, the PSWNN prediction accuracy respect to the WNN is improved from 1.7094 to 0.9889 meters for 10 seconds prediction and from 2.2652 to 1.8352 meters for 30 second prediction, respectively.

## 1. INTRODUCTION

During the past three decades, the Global Positioning System (GPS) has grown from a navigation concept through development and implementation to an operational system of 28 spacecraft currently serving millions of users. GPS has become an essential part of the navigation positioning, surveillance and timing aspects of ground, marine, aviation and space applications. The current uses, with new ones, will continue to grow resulting in a need for even more demanding capabilities (McDonald, 2002).

GPS measurements  $Z(t)$  can in general be written as:

$$Z(t) = P(t) + B(t) + W(t) \quad (1)$$

Where,  $P(t)$  is the geometrics range,  $B(t)$  is the measurement bias and  $W(t)$  is white noise. From equation (1) it can be seen that if the measurement bias and noise can be separated (or filtered) from the range, GPS data processing is relatively straightforward, because the receiver location can be easily obtained by a simple mapping from the measurement domain to the state domain. For reality the  $B(t)$  term includes several different bias sources which are mixed together and formed non-stationary and closed-correlated error. If the  $B(t)$  can be separated or eliminated from the remaining terms, then an unbiased and linear minimum variance estimation of the receiver location can be obtained by Least-Squares or Kalman filtering. However accurately modelling the bias in the time domain is not an easy task. The GPS biases and noise are time-variant. For example, multi-path, ionospheric delay and noise are satellite elevation dependent (Fu and Rizos, 1997).

Ranging errors are grouped into the six following classes:

- **Ephemeris Data:** Errors in the transmitted location of the satellite.
- **Satellite Clock:** Errors in the transmitted clock, including SA.
- **Ionosphere:** Errors in the corrections of pseudo-range caused by ionospheric effects.
- **Troposphere:** Errors in the corrections of pseudo-range caused by tropospheric effects.
- **Multipath:** Errors caused by reflected signals entering the receiver antenna.
- **Receiver:** Errors in the receiver's measurement of range caused by thermal noise, software accuracy, and interchannel biases.

Representative values for these errors are shown in Table 1 without SA. Consequently, the residual satellite clock error, at 2.1 m, is not the dominant error; in fact, the largest error is expected to be the mismodeling of the ionosphere, at 4.0 m. Thus, the worldwide civilian positioning error for GPS is potentially about 10 m (horizontal) and 13 m (vertical) (Parkinson, 1996).

| Error Source    | Bias | Random | Total |
|-----------------|------|--------|-------|
| Ephemeris Data  | 2.1  | 0.0    | 2.1   |
| Satellite Clock | 2.0  | 0.7    | 2.1   |
| Ionosphere      | 4.0  | 0.5    | 4.0   |
| Troposphere     | 0.5  | 0.5    | 0.7   |
| Multipath       | 1.0  | 1.0    | 1.4   |
| Receiver Noise  | 0.5  | 0.2    | 0.5   |

Table 1. Standard error model without SA (One-sigma error in m)

In order to increase standard GPS receiver's precision, one method is to introduce differential GPS (DGPS) technique. DGPS can reduce or cancel error sources such as satellite clock bias, atmosphere delays, and orbit bias. Differential corrections

could be computed at the reference station and were applied to the user's receiver with an update rate. Suggested DGPS update rates are usually less than twenty seconds. So, DGPS can remove common-mode errors of both the reference and user receivers. Errors are more often common when receivers are close together (less than 100 Km distances). Differential position accuracy of about 10 m is possible with DGPS based on C/A code GPS Standard Positioning Service (SPS) signals. It is necessary to notice that part of common-mode errors can not be compensated because of their random characteristics. Among of these errors random tropospheric delays, unmodeled ionosphere delays, multipath caused by reflected signals from surface near the receiver and receiver errors could be modelled (Ponomaryov and Pogrebnyak, 2000).

As stated above, the reference station DGPS connections measurements are received at the roving user with certain latency; some kind of extrapolator must therefore be implemented in order to predict the reference station measurements at the current epoch.

Recently neural networks have been established as a general approximation tool for fitting nonlinear models from input-output data. On the other hand, the recently introduced wavelet decomposition emerges as a new powerful tool for approximation. Such an approximation turns out to have a structure very similar to the one achieved by a (1+1/2)-layer neural network. In particular, recent advances have shown the existence of orthonormal wavelet bases, from which follows the availability of rates of convergence for approximation by wavelet based networks (Zhang and Benveniste, 1992).

This paper presents a short-term prediction of DGPS corrections based on the Parallel-Structure Wavelet Based Neural Networks (PSWNNs). The PSWNN consists of multiple WNNs connected in parallel. Each WNN predicts the same DGPS correction future values based on the past data with different time samples. The PSWNN decides the final predicted value as an average of each WNN outputs values.

This paper is organized as follow. Section II provides a brief introduction to wavelet, WNN, and PSWNN. Section III describes the proposed PSWNN architecture. Experiments are reported in section IV and finally conclusions are presented in section V.

## 2. DGPS CORRECTIONS PREDICTION

The DGPS corrections future value is represented by its previous data. If  $m\tau$  previous input data are given at  $k$ -th step, for a time series data  $x(k)$ , the  $\tau$ -step ahead value  $x(k + \tau)$  is expressed as (Kim and Kong, 1999; Mosavi, 2004):

$$x(k + \tau) = f[x(k), x(k - \tau), \dots, x(k - (m - 1)\tau)] \quad (2)$$

Where  $f[\cdot]$  denotes a function for time series prediction. Positive integer  $m$  refers to the embedding dimension and  $\tau$  is called time delay. Time series prediction is classified into one-step-ahead prediction and short-term prediction whether to use predicted value as input values or not. In one-step-ahead

prediction, the future data  $x(k + \tau)$  is predicted by its previous input values of the data sequence as equation (3):

$$\hat{x}(k + \tau) = f[\hat{x}(k), \hat{x}(k - \tau), \dots, \hat{x}(k - (m - 1)\tau)] \quad (3)$$

Future data in short-term prediction or long-term prediction are expressed according to the data previously predicted as in equation (4):

$$\hat{x}(k + \tau) = f[\hat{x}(k), \hat{x}(k - \tau), \dots, \hat{x}(k - (m - 1)\tau)] \quad (4)$$

## 3. PARALLEL STRUCTURE WAVELET BASED NEURAL NETWORKS

### 3.1 Wavelet

Wavelets are a family of orthonormal functions which are characterized by the translation and dilation of a single function  $\psi(x)$ . This family of functions, denoted by  $\psi_{m,k}(x)$  and given by:

$$\psi_{m,k}(x) = 2^{-\frac{m}{2}} \psi(2^m x - k) ; m, k \in Z \quad (5)$$

This function is a basis for the space of square integrable function  $L^2(R)$  i.e.:

$$f(x) = \sum_m \sum_k d_{m,k} \psi_{m,k}(x) \in L^2(R) \quad (6)$$

Wavelets are derived from scaling functions, i.e. functions which satisfy the recursion:

$$\varphi(x) = \sum_k a_k \varphi(2x - k) \quad (7)$$

In which a finite number of the filter coefficients  $a_k$  are non-zero. Any  $L^2(R)$  function  $f(x)$  may be approximated at resolution  $m$  by:

$$P_m(f)(x) = \sum_k c_{m,k} \varphi_{m,k}(x) ; k \in Z \quad (8)$$

Where,  $P_m(f)(x)$  represents the projection of the function  $f(x)$  onto the space of scaling functions at resolution  $m$ :

$$\varphi_{m,k}(x) = \varphi(2^m x - k) ; k \in Z \quad (9)$$

Which is a scaling function basis for scale  $m$  approximation of  $L^2(R)$ . The set of approximations  $P_m(f)(x)$  constitutes a multiresolution representation of the function  $f(x)$  (Maleknejad and Mesgarani, 2002).

### 3.2 Wavelet Neural Network

In these neural networks, the wavelet function replaces the role of sigmoid function in the hidden unit. The wavelet parameters and wavelet shape are adaptively computed to minimize an energy function for finding the optimal representation of the signal. Figure 1 presents a kind of three layers WNN structure with both "wavlon nonlinearity" and "sigmoid neuron nonlinearity" (Mosavi, 2004).

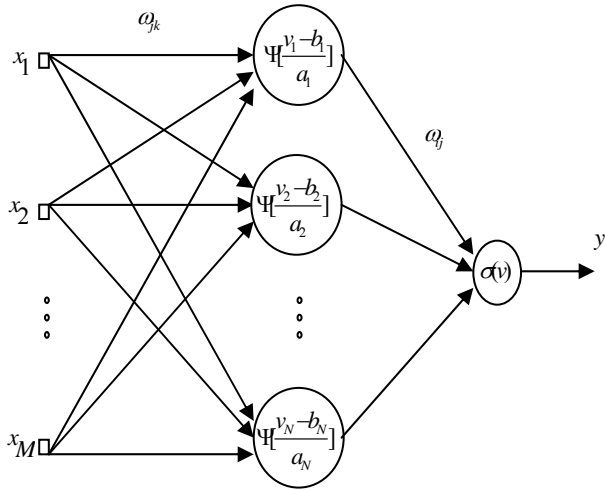


Figure 1. A three layers WNN

This network consists of three layers: an input layer, a hidden layer, and an output layer. The input layer has  $M$  nodes. The output layer also has only one neuron whose output is the signal represented by the weighted sum of several wavelets. The hidden layer is composed of a finite number of wavelets representing the signal.

### 3.2.1 Forward Calculations for WNN

Consider a network consisting of a total of  $N$  neurons in hidden layer with  $M$  external input connections (Figure 1). Let  $X(n)$  denotes the  $M - by - 1$  external input vector applied to the network,  $y(n)$  denotes the output of the network,  $w_{jk}(n)$  presents the weight between the hidden unit  $j$  and input unit  $k$ ,  $w_{ij}(n)$  denotes the connection weight between the output unit  $i$  and hidden unit  $j$ ,  $a_j(n)$  and  $b_j(n)$  present dilation and translation coefficients of wavlon in hidden layer at discrete time  $n$ , respectively.

The net internal activity of neuron  $j$  at time  $n$ , is given by:

$$v_j(n) = \sum_{k=0}^{k=M} w_{jk}(n).x_k(n) \quad (10)$$

Where,  $v_j(n)$  is the sum of inputs to the  $j - th$  hidden neuron,  $x_k(n)$  is the  $k - th$  input at time  $n$ . The output of the  $j - th$  neuron is computed by passing  $v_j(n)$  through the wavelets  $\psi_{a,b_j}(\cdot)$ , obtaining:

$$\psi_{a,b} [v_j(n)] = \psi \left[ \frac{v_j(n) - b_j(n)}{a_j(n)} \right] \quad (11)$$

The sum of inputs to the output neuron is obtained by:

$$v(n) = \sum_{j=0}^{j=N} w_{ij}(n).\psi_{a,b} [v_j(n)] \quad (12)$$

The output of the network is computed by passing  $v(n)$  through the nonlinear function  $\sigma(\cdot)$ , obtaining:

$$y(n) = \sigma[v(n)] \quad (13)$$

### 3.2.2 Learning Algorithm for WNN

The instantaneous sum of squared error at time  $n$  as:

$$E(n) = \frac{1}{2} e^2(n) = \frac{1}{2} [y(n) - d(n)]^2 \quad (14)$$

Where,  $d(n)$  denote the desired response of output at time  $n$ . To minimize of above cost function, the method of steepest descent is used. The weight between the hidden unit  $j$  and input unit  $k$  can be adjusted according to:

$$\begin{aligned} \Delta w_{jk}(n+1) &= -\eta \cdot \frac{\partial E(n)}{\partial w_{jk}(n)} + \mu \Delta w_{jk}(n) \\ &= \eta \cdot e(n) \cdot \sigma'[v(n)] \cdot w_{ij}(n) \cdot \psi_{a,b}' [v_j(n)]. \end{aligned} \quad (15)$$

$$\frac{x_k(n)}{a_j(n)} + \mu \Delta w_{jk}(n)$$

Where,  $\eta$  is a learning rate. The connection weight between the output unit  $i$  and hidden unit  $j$  is updated as follow:

$$\begin{aligned} \Delta w_{ij}(n+1) &= -\eta \cdot \frac{\partial E(n)}{\partial w_{ij}(n)} + \mu \Delta w_{ij}(n) \\ &= \eta \cdot e(n) \cdot \sigma'[v(n)] \cdot \psi_{a,b}' [v_j(n)] + \mu \Delta w_{ij}(n) \end{aligned} \quad (16)$$

The translation coefficient of the  $j - th$  wavlon in hidden layer can be adjusted according to:

$$\begin{aligned} \Delta b_j(n+1) &= -\eta \cdot \frac{\partial E(n)}{\partial b_j(n)} + \mu \Delta b_j(n) \\ &= -\eta \cdot e(n) \cdot \sigma'[v(n)] \cdot w_{ij}(n) \cdot \psi_{a,b}' [v_j(n)] \\ &\quad \cdot \frac{1}{a_j(n)} + \mu \Delta b_j(n) \end{aligned} \quad (17)$$

The dilation coefficient of the  $j - th$  wavlon in hidden layer is updated as follow:

$$\begin{aligned} \Delta a_j(n+1) &= -\eta \cdot \frac{\partial E(n)}{\partial a_j(n)} + \mu \Delta a_j(n) \\ &= -\eta \cdot e(n) \cdot \sigma'[v(n)] \cdot w_{ij}(n) \cdot \psi_{a,b}' [v_j(n)] \\ &\quad \cdot \frac{v_j(n) - b_j(n)}{a_j(n)^2} + \mu \Delta a_j(n) \end{aligned} \quad (18)$$

The wavelet function which we have considered here is the so called "Gaussian-derivative" function as:

$$\psi(x) = -x \cdot e^{-\frac{1}{2} \cdot x^2} \quad (19)$$

The usual sigmoid function of used in this research is as follow:

$$\sigma(x) = \frac{1}{1 + e^{-x}} \quad (20)$$

### 3.2.3 WNN Predictor

Work in WNNs has concentrated on forecasting future developments of DGPS corrections from values of  $x$  up to the current time. The proposed WNN in this research is shown in Figure 2. The choice of the WNN parameters is also important. In this paper, the order was based on the experimental results.

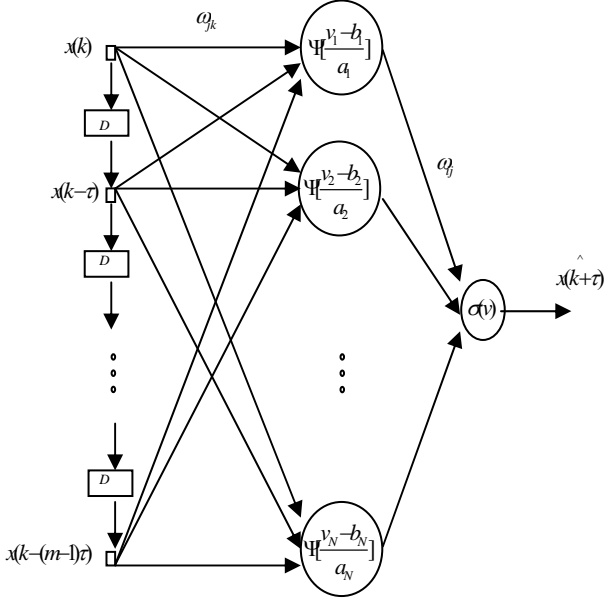


Figure 2. A proposed WNN for DGPS correction prediction

### 3.3 Wavelet Neural Network of Parallel-Structure

The PSWNN consists of multiple number of the WNN connected in parallel for predicting time series. Figure 3 shows the structure of the Parallel-Structure WNN. The PSWNN contains  $N$  WNNs as  $WNN_1, WNN_2, \dots, WNN_N$  connected in parallel. Each WNN produces predicted value for the the same time index  $k+r$ . With a decision scheme, the PSWNN outputs the final predicted value  $\hat{x}(k+r)$ .

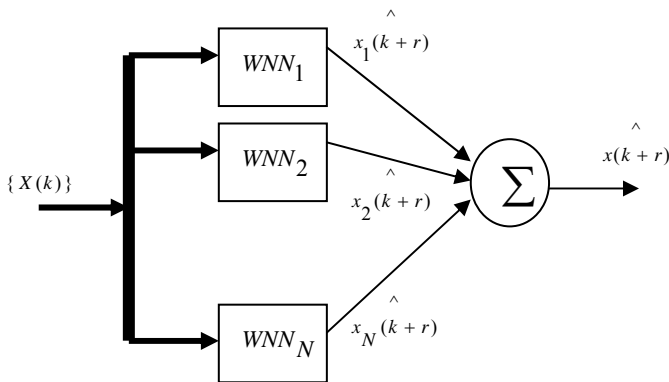


Figure 3. The PSWNN structure

Time series prediction with the PSWNN is characterized by the parameters  $\tau$  and  $m$ . The embedding dimension  $m$  defines the number of inputs to the WNN, and the value  $\tau$  defines the time interval of input data. The  $p$ -th WNN ( $WNN_p$ ) in the PSWNN takes time delay as  $\tau = p$  and different  $m$ .

Consider the PSWNN for predicting  $x(k+r)$ , the future data at  $(k+r)$ -th time step. The  $p$ -th WNN predicts value  $\hat{x}_p(k+r)$  based on its previous data  $\hat{x}(k+r-p)$ ,  $\hat{x}(k+r-2p)$ , ..., and  $\hat{x}(k+r-mp)$ . The PSWNN determines the final predicted value  $\hat{x}(k+r)$  from the outputs  $\hat{x}_1(k+r), \hat{x}_2(k+r), \dots, \hat{x}_N(k+r)$  of each WNN. The PSWNN determines the final predicted value  $\hat{x}(k+r)$  as the average of each WNN as follow:

$$\hat{x}(k+r) = \frac{1}{N} \sum_{i=1}^N \hat{x}_i(k+r) \quad (21)$$

For example, consider the PSWNN with three WNN ( $N=3$ ). If the values  $m$  of each WNN are chosen as 3, 4, and 3, then the  $(\tau, m)$  pairs become (1,3) for  $WNN_1$ , (2,4) for  $WNN_2$ , and (3,3) for  $WNN_3$ , respectively. Figure 4 shows the input

data used to predict the future data  $\hat{x}(k+r)$  using the PSWNN.  $WNN_1$  Predicts  $\hat{x}_1(k+r)$  using inputs  $x(k)$ ,  $x(k-r)$ , and  $x(k-2r)$ . Also,  $WNN_2$  outputs  $\hat{x}_2(k+r)$  using inputs  $x(k-r)$ ,  $x(k-3r)$ , and  $x(k-5r)$ . Finally,  $WNN_3$  predicts  $\hat{x}_3(k+r)$  using inputs  $x(k-2r)$ ,  $x(k-5r)$ , and  $x(k-8r)$ .

|         | $x(k-8r)$ | $x(k-7r)$ | $x(k-6r)$ | $x(k-5r)$ | $x(k-4r)$ | $x(k-3r)$ | $x(k-2r)$ | $x(k-r)$ | $x(k)$ | $\hat{x}(k+r)$   |
|---------|-----------|-----------|-----------|-----------|-----------|-----------|-----------|----------|--------|------------------|
| $WNN_1$ | 0         | 0         | 0         | 0         | 0         | 0         | ●         | ●        | ●      | $\hat{x}_1(k+r)$ |
| $WNN_2$ | 0         | ●         | 0         | ●         | 0         | ●         | 0         | ●        | 0      | $\hat{x}_2(k+r)$ |
| $WNN_3$ | ●         | 0         | 0         | ●         | 0         | 0         | ●         | 0        | 0      | $\hat{x}_3(k+r)$ |

Figure 4. Input data to each WNN in an sample PSWNN ( $r=1$ )

#### 4. EXPERIMENT

Performance of the proposed WNN and PSWNN were evaluated by data sets that were collected in the Iran University of Science and Technology. Figure 5, Figure 6, and Figure 7 show  $D_x$ ,  $D_y$  and  $D_z$  predictions for 100 test data by using proposed WNNs ( $M = 3, N = 3$ , and  $SA = off$ ).

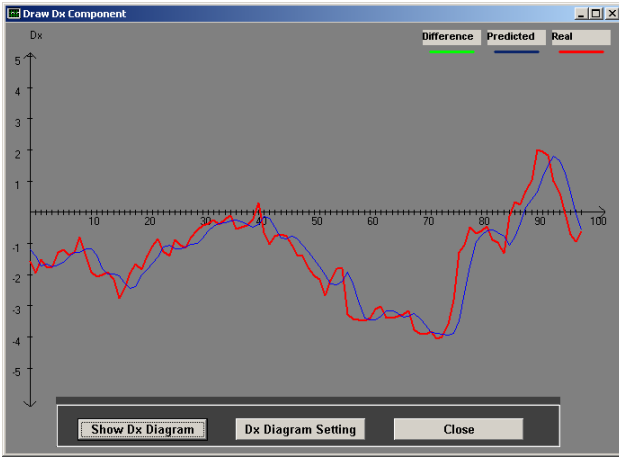


Figure 5.  $D_x$  predictions by using proposed WNN



Figure 6.  $D_y$  predictions by using proposed WNN

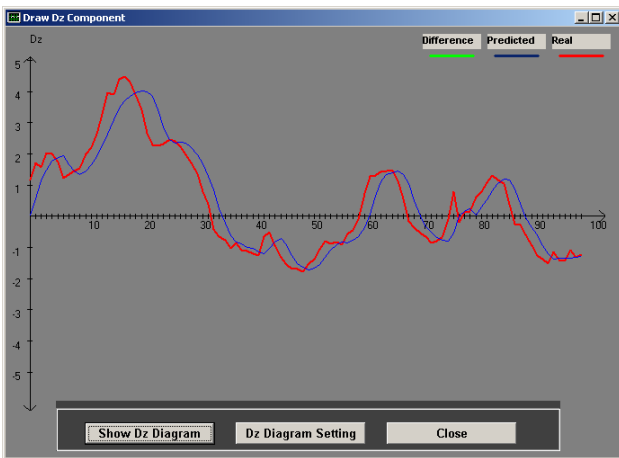


Figure 7.  $D_z$  predictions by using proposed WNN

Also, Figure 8, Figure 9, and Figure 10 show  $D_x$ ,  $D_y$  and  $D_z$  predictions for 100 test data by using proposed

PSWNNs with three WNNs as (1,3) for  $WNN_1$ , (2,4) for  $WNN_2$ , and (3,3) for  $WNN_3$ , respectively.



Figure 8.  $D_x$  predictions by using proposed PSWNN



Figure 9.  $D_y$  predictions by using proposed PSWNN

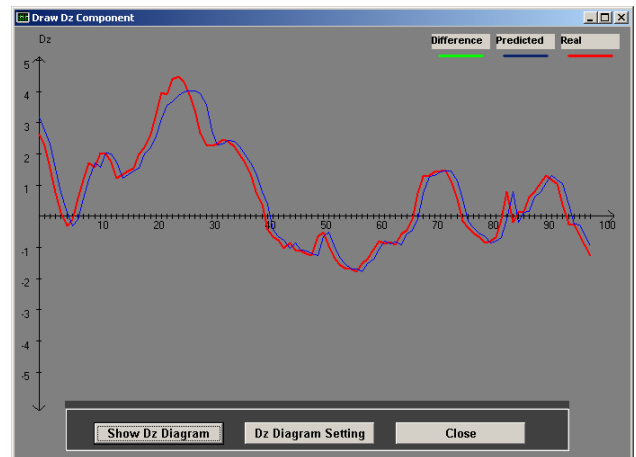


Figure 10.  $D_z$  predictions by using proposed PSWNN

#### 4.1 Test Setup Description

Figure 11 shows DGPS test setup. Both the reference station GPS and the mobile unit GPS receive signals from the same satellite. The GPS receivers, the computers for data visualization and recording and also the radio modem for the

reception of the DGPS correction data were integrated inside the reference station and the mobile unit.

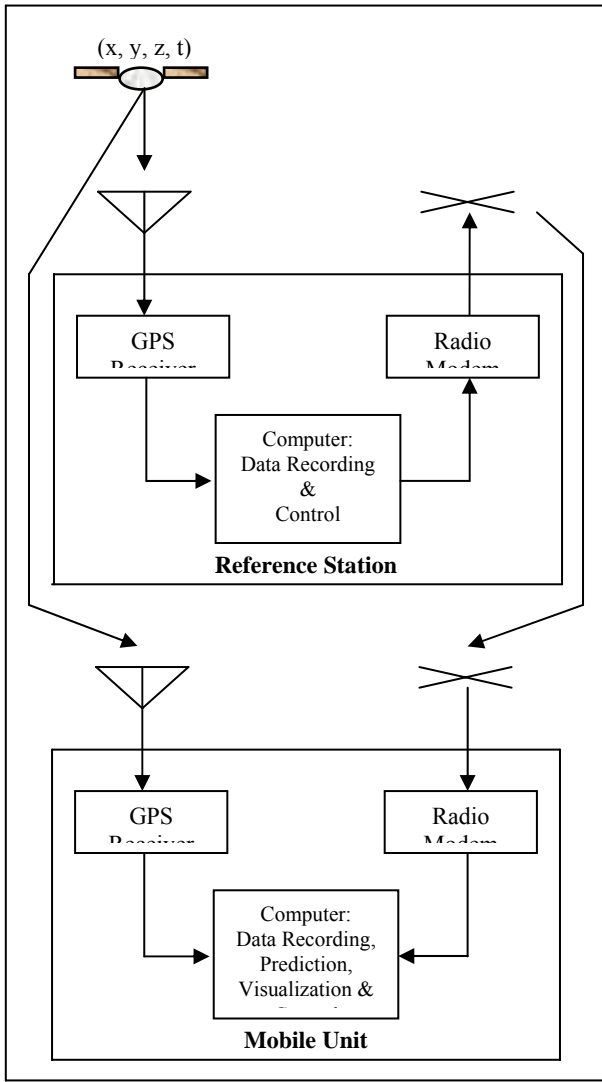


Figure 11. DGPS test setup

Two low cost GPS engine manufactured by Rockwell Company were used. The Rockwell “MicroTraker Low Power (MLP)” receiver is a single board, five parallel-channels, and L1-only Coarse Acquisition (C/A) code capability. One receiver was operated with a passive patch antenna; the other was operated with an active patch antenna which means that there is a low noise preamplifier integrated in the antenna which is powered by the receiver via the RF cable.

The commanding of the receivers and the data visualization and recording was done with the developed software by paper author on a notebook computer with a serial interface. All the computer programs were coded in C-language and visual basic 6.

The antenna reference position was determined with “Average Mode” of the developed software which means that the average of the position solutions was determined over one hour. With this averaged position the receiver was set in “Fix Position Mode” and the output of correction data was started.

For the transmission of the DGPS corrections data from the reference station to the mobile unit, a radio modem was used on

both sides with one transmission channel on a UHF frequency, MSK modulation and 5 W transmitter powers. The received DGPS corrections data via the radio data link were fed to the serial interface in the mobile unit. The last valid positions are used for extrapolating the position. Figure 12 shows the developed hardware of this research.



Figure 12. The developed hardware of this research

#### 4.2 Experimental Results

In order to analyze the DGPS position accuracy, we used Root Mean Square (RMS) as below (Sang, 1997):

$$RMS = \sqrt{\frac{1}{M} \sum_{i=1}^{i=M} (d_i - y_i)^2} \quad (22)$$

Where,  $M$  is test numbers,  $d_i$  denotes the desired response of output, and  $y_i$  presents the NNs output at test  $i$ . Optimal value of  $m$  and  $\tau$  are determined when the prediction error RMS is the smallest value of one-step-ahead prediction. In experiments, the optimal value of  $m$  for prediction using a single WNN becomes 3. Also as shown in Figure 13, the optimal value of  $(\tau, m)$  pairs in prediction using PSWNN with three WNNs obtain as (1,3) for  $WNN_1$ , (2,4) for  $WNN_2$ , and (3,3) for  $WNN_3$ , respectively.

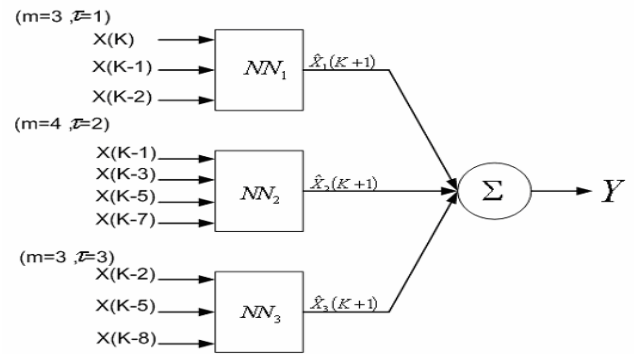


Figure 13. PSWNN with three WNNs as (1,3) for  $NN_1$ , (2,4)

for  $NN_2$ , and (3,3) for  $NN_3$ , respectively

Figure 14, Figure 15, and Figure 16 show  $D_x$ ,  $D_y$  and  $D_z$  predictions for 2000 test data by using proposed PSWNNs of Figure 13.

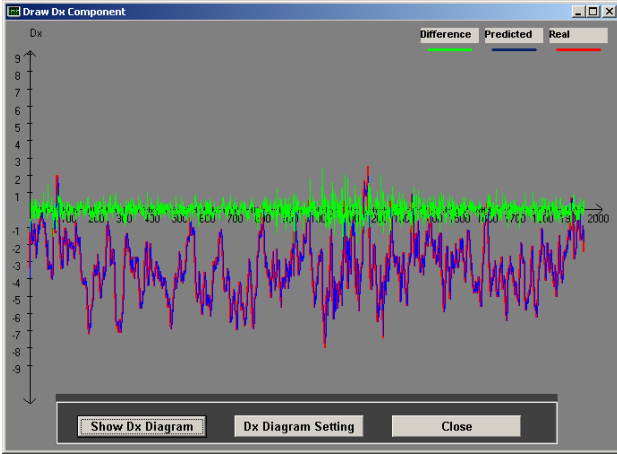


Figure 14.  $D_x$  predictions by using PSWNN of Figure 13

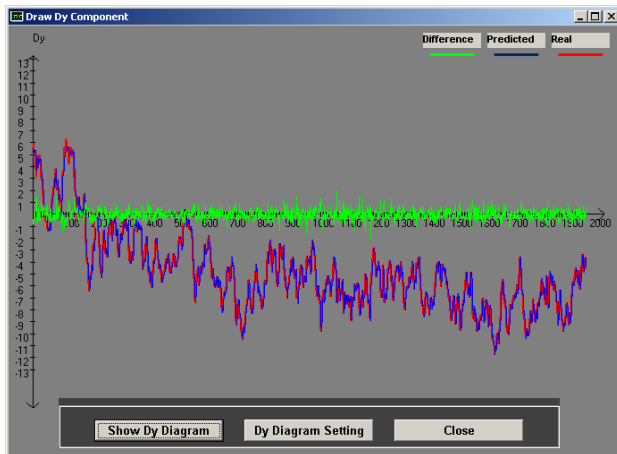


Figure 15.  $D_y$  predictions by using PSWNN of Figure 13

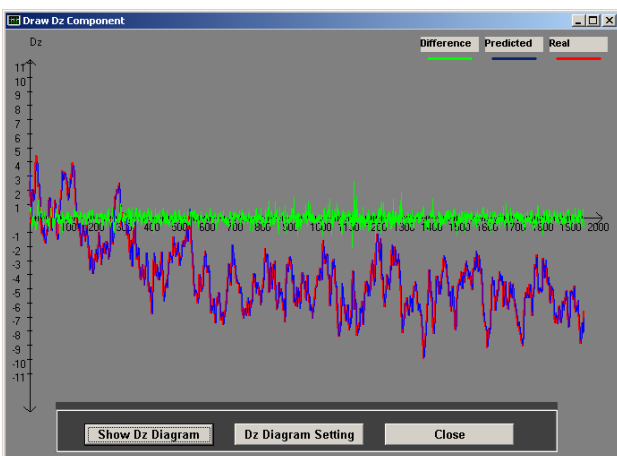


Figure 16.  $D_z$  predictions by using PSWNN of Figure 13

Table 2 to Table 3 show statistical significance characteristics of one-step-ahead prediction errors (the difference between the predicted and real values) for 1000 test data using WNNs and PSWNNs, respectively.

| Parameters         | X Component      | Y Component      | Z Component      |
|--------------------|------------------|------------------|------------------|
| Max                | 1.4934130        | 1.5420700        | 1.4976000        |
| Min                | -1.9666767       | -1.6185998       | -1.4473175       |
| <b>RMS</b>         | <b>0.3594700</b> | <b>0.4059940</b> | <b>0.3564420</b> |
| Average            | -0.0032720       | 0.0099290        | 0.0083180        |
| Variance           | 0.0001290        | 0.0001650        | 0.0001270        |
| Standard Deviation | 0.0113730        | 0.0128410        | 0.0112740        |

Table 2. Prediction Errors Statistical Significance Characteristics Using WNNs (SA off)

| Parameters         | X Component      | Y Component      | Z Component      |
|--------------------|------------------|------------------|------------------|
| Max                | 1.4934130        | 1.5420700        | 1.4976000        |
| Min                | -1.9666767       | -1.6185998       | -1.4473175       |
| <b>RMS</b>         | <b>0.3554200</b> | <b>0.4055010</b> | <b>0.3546820</b> |
| Average            | -0.0000440       | 0.0104800        | 0.0046190        |
| Variance           | 0.0001260        | 0.0001640        | 0.0001260        |
| Standard Deviation | 0.0112450        | 0.0128250        | 0.0112210        |

Table 3. Prediction Errors Statistical Significance Characteristics Using PSWNN (SA off)

As shown in Table 2 and Table 3, the PSWNNs respect to WNNs has greater accuracy for DGPS corrections prediction. Also, the WNNs and PSWNNs were trained to predict the DGPS corrections 10 and 30 seconds ahead of the current epoch. The obtained results are shown in Table 4 and Table 5, respectively.

| Algorithm    | Total RMS Error |
|--------------|-----------------|
| <b>WNN</b>   | 1.7094          |
| <b>PSWNN</b> | 0.9889          |

Table 4. Total RMS error of position components for 10 seconds ahead prediction

| Algorithm    | Total RMS Error |
|--------------|-----------------|
| <b>WNN</b>   | 2.2652          |
| <b>PSWNN</b> | 1.8352          |

Table 5. Total RMS error of position components for 30 seconds ahead prediction

As shown in Table 3 and Table 4, the PSWNNs respect to WNNs has greater accuracy for DGPS corrections prediction.

## 5. CONCLUSIONS

This paper has presented WNN and PSWNN architecture and also these training algorithms for DGPS corrections prediction. The PSWNN consists of multiple numbers of WNNs connected in parallel. Each WNN in the PSWNN predicts the same DGPS corrections future value at the same time index with different embedding dimension and time delay. The embedding dimension was chosen optimally to have superior performance for each time delay value. The PSWNN determines the final predicted value by averaging the outputs of each WNN. The performance of proposed PSWNN was compared with WNN in application of DGPS corrections prediction. The proposed algorithms in DGPS system were implemented by a low cost commercial Coarse/Acquisition (C/A) code GPS module. The experimental test results with real data emphasize which the PSWNN has great approximation ability and suitability in DGPS connection prediction than WNN; so that, the PSWNN prediction accuracy respect to the WNN was improved from 1.7094 to 0.9889 meters for 10 seconds prediction and from 2.2652 to 1.8352 meters for 30 second prediction, respectively. An additional advantage of the investigated DGPS using proposed NNs prediction is their low cost because of using only commercial C/A code GPS modules for the reference and users.

## References

- Fu, W.X., and Rizos, C., 1997. The applications of wavelets to GPS signal processing. In: *10th International Technical Meeting of the satellite Division of the U.S. Institute of Navigation*, 16-19 September, Kansas City, Missouri, pp. 697-703.
- Kim, M.S., and Kong, S.G., 1999. Time series prediction using the parallel-structure fuzzy system. In: *IEEE Conference on Fuzzy Systems*, 22-25 August, Seoul, Korea, 2, pp. 934-938.
- McDonald, K.D., 2002. The modernization of GPS: plans, new capabilities and the future relationship to Galileo. *Journal of Global Positioning System*, 1(1), pp. 1-17.
- Maleknejad, K., Mesgarani, H., and Nikazad, T., 2002. Wavelet-galerkin solutions for fredholm integral equations. *International Journal of Engineering Science, Iran University of Science and Technology*, 13(5), pp. 75-80.
- Mosavi, M.R., Mohammadi, K., and Refan, M.H., 2004. A new approach for improving of GPS positioning accuracy by using an adaptive neurofuzzy system, before and after S/A is turned off. *International Journal of Engineering Science, Iran University of Science and Technology*, 15(1), pp. 101-114.
- Mosavi, M.R., 2004. A wavelet based neural network for DGPS corrections prediction. *WSEAS Transactions on Systems*, 3(10), pp. 3070-3075.
- Parkinson, B.W., Spilker, J.J., Axelrad, P., and Enge, P., 1996. Global positioning system: theory and applications. *The American Institute of Aeronautics and Astronautics*, pp. 478-483.
- Ponometryov, V.I., Pogrebnyak, O.B., Rivera, L.N., and Garcia, J.C.S., 2000. Increasing the accuracy of differential global positioning system by means of use the Kalman filtering technique. In: *International Symposium on Industrial Electronics*, 4-8 December, Cholula, Puebla, Mexico, 2, pp. 637-642.
- Sang, J., Kubik, K., and Zhang, L., 1997. Prediction of DGPS corrections with neural networks. In: *IEEE Conference on Knowledge-Based Intelligent Electronic Systems*, 21-23 May, Adelaide, Australia, pp. 355-361.
- Zhang, Q., and Benveniste, A., 1992. Wavelet networks. *IEEE Transaction on Neural Networks*, 3(6), pp. 889-898.